Insect Biochemistry and Molecular Biology 110 (2019) 52–59

Contents lists available at ScienceDirect

Insect Biochemistry and Molecular Biology

journal homepage: www.elsevier.com/locate/ibmb

Two functionally distinct CYP4G genes of *Anopheles gambiae* contribute to cuticular hydrocarbon biosynthesis

Mary Kefi[a,b], Vasileia Balabanidou[a], Vassilis Douris[a], Gareth Lycett[c], René Feyereisen[d], John Vontas[a,e,*]

[a] Institute of Molecular Biology and Biotechnology, Foundation for Research and Technology-Hellas, 73100, Heraklion, Greece
[b] Department of Biology, University of Crete, VassilikaVouton, 71409, Heraklion, Greece
[c] Department of Vector Biology, Liverpool School of Tropical Medicine, Liverpool, L3 5QA, United Kingdom
[d] Department of Plant and Environmental Sciences, University of Copenhagen, Copenhagen, 1017, Denmark
[e] Pesticide Science Laboratory, Department of Crop Science, Agricultural University of Athens, 11855, Athens, Greece

ARTICLE INFO

Keywords:
Anopheles gambiae
CYP4Gs
P450 decarbonylase
Oenocytes
Cuticular hydrocarbons (CHCs)

ABSTRACT

Cuticular hydrocarbon (CHC) biosynthesis is a major pathway of insect physiology. In *Drosophila melanogaster* the cytochrome P450 CYP4G1 catalyses the insect-specific oxidative decarbonylation step, while in the malaria vector *Anopheles gambiae*, two CYP4G paralogues, CYP4G16 and CYP4G17 are present. Analysis of the subcellular localization of CYP4G17 and CYP4G16 in larval and pupal stages revealed that CYP4G16 preserves its PM localization across developmental stages analyzed; however CYPG17 is differentially localized in two distinct types of pupal oenocytes, presumably oenocytes of larval and adult developmental specificity. Western blot analysis showed the presence of two CYP4G17 forms, potentially associated with each oenocyte type. Both *An. gambiae CYP4Gs* were expressed in *D. melanogaster* flies in a *Cyp4g1* silenced background in order to functionally characterize them *in vivo*. *CYP4G16*, *CYP4G17* or their combination rescued the lethal phenotype of *Cyp4g1*-knock down flies, demonstrating that CYP4G17 is also a functional decarbonylase, albeit of somewhat lower efficiency than CYP4G16 in *Drosophila*. Flies expressing mosquito CYP4G16 and/or CYP4G17 produced similar CHC profiles to 'wild-type' flies expressing the endogenous CYP4G1, but they also produce very long-chain dimethyl-branched CHCs not detectable in wild type flies, suggesting that the specificity of the CYP4G enzymes contributes to determine the complexity of the CHC blend. In conclusion, both *An. gambiae* CYP4G enzymes contribute to the unique *Anopheles* CHC profile, which has been associated to defense, adult desiccation tolerance, insecticide penetration rate and chemical communication.

1. Introduction

Insect cuticular hydrocarbons (CHCs) are a complex blend of long-chain alkanes or alkenes and methyl-branched alkanes that act as essential waterproofing components of the insect epicuticular layer to prevent desiccation, and/or serve as species- and sex-specific semiochemicals (Arcaz et al., 2016; Chung and Carroll, 2015; Cocchiararo-Bastias et al., 2011; Gibbs, 2011; Howard and Blomquist, 2005). Although CHC profiles differ among insect species, the main biosynthetic pathway is conserved (Howard and Blomquist, 2005). Their synthesis from fatty acids requires a suite of elongases, desaturases and acyl-CoA reductases that function in concert in large, ectodermally derived cells, called oenocytes (Fan et al., 2003). An additional enzyme required for the final step of CHC synthesis, a cytochrome P450 of the CYP4G subfamily was identified as oxidative decarbonylase (Qiu et al., 2012). *Drosophila* CYP4G1 is highly expressed in oenocytes together with NADPH cytochrome P450 reductase (CPR) and catalyses the oxidative decarbonylation of long-chain aldehydes (Qiu et al., 2012). Oenocyte-specific RNAi-mediated knock down of CYP4G1 results in severe susceptibility to desiccation, conferring high mortality at emergence (Qiu et al., 2012). The CYP4G P450 subfamily is evolutionarily conserved across insects (Feyereisen, 2006) but is absent in other orders, such as crustaceans and chelicerates. This may indicate an essential function of *CYP4G* genes specific to insects, suggested to be a key to success in terrestrial adaptation. Insect genomes sequenced so far possess at least one CYP4G (one in honey bee and aphid, two in *Drosophila* and several mosquito species) (Qiu et al., 2012).

Several earlier studies indicate distinct lipid/CHC signatures across

* Corresponding author. Institute of Molecular Biology and Biotechnology, Foundation for Research and Technology-Hellas, 73100, Heraklion, Greece.
E-mail address: vontas@imbb.forth.gr (J. Vontas).

https://doi.org/10.1016/j.ibmb.2019.04.018
Received 12 February 2019; Received in revised form 21 April 2019; Accepted 29 April 2019
Available online 30 April 2019
0965-1748/

development. Firstly, the necessary renewal of the cuticular lipids at each molt (Wigglesworth, 1988) implies distinct lipids and presumably differences in their CHC derivatives at different developmental stages. Secondly, aquatic insects should prevent liquid entry into the tracheal system while apart from this terrestrial insects must be protected from desiccation which means they should prevent water loss. Adult *An. gambiae* and *D. melanogaster* with their early developmental stages being aquatic or semi-aquatic respectively (Parvy et al., 2012) presumably reflect the distinct needs in lipids/hydrocarbons through development. Larval oenocytes synthesize very-long-chain fatty acids (VLCFA) which are accumulated into spiracles, the organs controlling the entry of air into the trachea, protecting respiratory system from liquid entry (Parvy et al., 2012). Oenocyte-specific RNAi-based knock down of *Cyp4g1* or *Cpr* in larvae and adults results in severe depletion in epicuticular HC in the few adult survivors. The majority die at eclosion presumably of extreme sensitivity to desiccation at the time of adult emergence (Qiu et al., 2012). Furthermore, pheromone-driven courtship was altered in *Cyp4g1*-KD CHC depleted females (Qiu et al., 2012). Similar phenotypes are produced when oenocytes are specifically ablated in adult *Drosophila* females.

Underlying this phenotype is the presence of two different oenocyte cells in larvae and adults that have separate developmental origins (Billeter et al., 2009; Gutierrez et al., 2007; Makki et al., 2014) and have been described in mosquitoes (Lycett et al., 2006) and other Diptera (Makki et al., 2014). Overall, these latter studies suggest that presumably larval oenocytes have a primary role in CHC production during molting and water-loss prevention in the tracheal system, while CHCs produced from adult oenocytes are mostly implicated in sex- and species-specificity, pheromonal communication and desiccation resistance (Makki et al., 2014; Parvy et al., 2012).

The fact that *An. gambiae* oenocytes express two CYP4Gs (CYP4G16 and CYP4G17) as opposed to the single CYP4G expressed in *D. melanogaster* oenocytes is possibly indicative of a functional diversity. A recent study has shown that CYP4G16 is bound on the periphery of adult oenocytes, while CYP4G17 is dispersed among the cytoplasm (Balabanidou et al., 2016). In addition, *in vitro* experiments indicate the ability of CYP4G16 to catalyze the conversion of long-chain aldehydes to hydrocarbons, hence completing the final biosynthetic step, whereas the role of CYP4G17 remains unknown (Balabanidou et al., 2016). While CYP4G16 was able to convert C18 aldehyde to HC, no such activity could be demonstrated for CYP4G17 which was not expressed well *in vitro* and for which longer aldehydes could not be tested because of solubility issues (Balabanidou et al., 2016). A recent study in *Dendroctonus ponderosae* showed that shorter-chain alcohols can also be substrates of CYP4Gs (MacLean et al., 2018), which can thus serve in the biosynthesis of the pine beetle pheromone exo-brevicomin as well as in CHC biosynthesis.

The variation in insect CHC blend has been associated with physiological adaption to ecological and reproductive parameters (Chung and Carroll, 2015). Indeed, methyl-branched CHCs have been shown to affect both waterproofing and mating in *Drosophila serrata* (Chung et al., 2014). It is likely that longer carbon chains in CHCs increase the melting temperature of the insect epicuticular wax layer and probably influence desiccation resistance, and methyl branching increases the chemical information of the cuticle (Chung and Carroll, 2015). Some studies have indicated that *An. gambiae* is rich in methyl-branched very long chain CHCs (mono- or dimethyl) (Balabanidou et al., 2016; Caputo et al., 2005), which could potentially serve both biological functions.

Moreover, cuticular analysis of an insecticide resistant *An. gambiae* population compared to a susceptible one, revealed a thicker epicuticle, the major deposition site of CHCs, in the femur leg segment, thus creating a thicker hydrophobic barrier to insecticide molecules, as shown by reduced penetration rate of radiolabeled insecticide (Balabanidou et al., 2016). The higher CHC amount is in line with the overexpression of CYP4Gs in the resistant mosquitoes (Balabanidou et al., 2016), implicating an additional role of CHCs in insecticide penetration resistance (Balabanidou et al., 2018).

In this study, the subcellular localization of *An. gambiae* CYP4Gs was analyzed in oenocytes from earlier developmental stages, i.e. 4th instar larvae and pupae. Furthermore, functional analysis of the *An. gambiae* CYP4Gs was performed *in vivo* using GAL4/UAS heterologous expression coupled with RNAi knock-down of the endogenous *Cyp4g1* gene in *Drosophila melanogaster* and the ability of CYP4G16 and/or CYP4G17 in different doses and in combination to rescue the lethal (*Cyp4g1* Knock-down) phenotype. CHC analysis of the rescued flies then gave insights into the catalytic efficiency and specificity of the two anopheline CYP4Gs in a *Drosophila* background.

2. Materials and methods

2.1. Mosquito strains

The *An. gambiae* N'Gousso strain was reared under standard insectary conditions at 27 °C and 70–80% humidity under a 12:12 h photoperiod. The strain is originally from Cameroon and is susceptible to all classes of insecticide (Edi et al., 2012).

2.2. Antibodies

Rabbit polyclonal antibodies targeting CYP4G16 have previously been developed (Balabanidou et al., 2016). The specific antibodies that were used for the detection of CYP4G17 (AGAP000877) have previously been described (Ingham et al., 2014). The epitopes recognize residues 231–312 and 233–315 of CYP4G16 and CYP4G17 respectively.

2.3. Preparation of cryosections for immunohistochemistry, immunofluorescence and microscopy

4th instar *An. gambiae* larvae and dissected pupal abdomens were fixed in cold solution of 4% PFA (methanol free, Thermo scientific) in phosphate-buffered saline (PBS) for 4 h, cryo-protected in 30% sucrose/PBS at 4 °C for 12 h, immobilized in Optimal Cutting Temperature O.C.T. (Tissue-Tek, SAKURA) and stored at −80 °C until use. Immunofluorescence analysis, followed by confocal microscopy, was performed on longitudinal sections of the frozen larval and pupal specimens as described previously (Ingham et al., 2014). Briefly, 7 µm sections, obtained in cryostat with UVC disinfection (Leica CM1850UV) were washed (3 × 5 min) with 0,05% Tween in PBS and blocked for 3 h in blocking solution (1% Fetal Bovine Serum, biosera, in 0,05% Triton/PBS). Then, the sections were stained with rabbit primary antibodies in 1/500 dilution, followed by goat anti-rabbit (Alexa Fluor 405, Molecular Probes) (1/1000) that gave the cyan color. Also To-PRO 3-Iodide (Molecular Probes), which specifically stains DNA (red color), was used, after RNAse A treatment. Finally, images were obtained on a Leica SP8 laser-scanning microscope, using the 40-objective.

2.4. Topology experiments: predictions and whole mounts (preparation of abdominal walls for immunohistochemistry and immunofluorescence)

The predicted membrane topology of both *An. gambiae* CYP4Gs was analyzed using Phobius, a transmembrane topology and signal peptide predictor program (Kall et al., 2007). For whole-mount larval abdomen immunostaining, abdominal walls from 4th instar larvae were dissected and fixed for 30 min at room temperature in 4% methanol-free formaldehyde (Thermo Scientific) in PBS supplemented with 2 mM $MgSO_4$ and 1 mM EGTA, washed for 5 min with PBS, and then washed with methanol for precisely 2 min. After methanol wash, the tissues were washed again with PBS and then blocked for 1 h in blocking solution (bl sol: 1% BSA, 0.1% Triton X-100 in PBS). Then the tissues were stained with rabbit primary antibodies in 1/500 dilution in the blocking solution, followed by goat anti-rabbit antibody (Alexa-Fluor 488; Molecular Probes; 1:1000) that gave the green color. Up to this point the same

protocol omitting the addition of Triton was used to create the non-permeabilized conditions. Finally, DNA was stained red with ToPRO 3-Iodide (Molecular Probes). Pictures were obtained on Leica M205 FA Fluorescent Stereomicroscope.

2.5. Fly strains

In order to drive oenocyte–specific expression, the RE-Gal4 driver line ((Bousquet et al., 2012); kindly provided by Jean-Francois Ferveur, Université de Bourgogne, Dijon, France) was employed. This line contains the RE fragment of the *desat1* gene promoter, whose expression is mostly confined to oenocytes in *Drosophila* adults, (though some expression is also observed in accessory glands in males (Bousquet et al., 2012)). The responder strain UAS-Cyp4g1-KD (#102864 KK from Vienna Drosophila Resource Center) was used for RNAi mediated knock-down of CYP4G1.

2.6. Generation of UAS responder flies

Since both the RE-Gal4 driver and UAS-Cyp4g1-KD responder transgenes are located on *Drosophila* chromosome 2, the two 'mosquito CYP4G' responder fly strains were generated by φC31 integrase mediated attB insertion (Groth et al., 2004) using landing site VK13 in chromosome 3 to facilitate downstream manipulations. Two *ad hoc* integration vectors were generated by modifying the vector dPelican.attB.UAS_CYP6A51 (Tsakireli et al., 2019). This plasmid is a modification of a vector based on pPelican (Barolo et al., 2000) which contains *gypsy* insulator sequences flanking the expression cassette (Piwko et al., 2019); plasmid #30)). Kapa Taq DNA Polymerase (Kapa Biosystems) was used for the amplification of a 1713 bp fragment containing *CYP4G16* ORF using primer pair CYP4G16F/CYP4G16R (Table S1) that introduce a 5′ BssHII site and a 3′ XhoI site, while primer pair CYP4G17F/CYP4G17R (Table S1) was used to amplify a 1711 bp fragment containing the *CYP4G17* ORF and introducing a 5′ AscI and a 3′ SalI, respectively. The templates for the amplification of CYP4G16 and CYP4G17 ORFs were cDNAs of adult mosquito RNAs. PCR conditions were 95 °C for 3 min, followed by 35 cycles of 95 °C for 30 s, 50 °C for 30 s, 72 for 2 min. The amplicons were purified, digested with the relevant enzyme combinations (BssHII/XhoI for *CYP4G16* fragment and AscI/SalI for *CYP4G17* fragment) and subcloned into the unique MluI/XhoI sites of dPelican.attB.UAS_CYP6A51 (Tsakireli et al., 2019) so that the existing ORF is removed and replaced by the *CYP4G16* or *CYP4G17* ORFs downstream of the 5xUAS-promoter sequence and just upstream of the SV40 polyadenylation sequence. Each *de novo* UAS expression recombinant plasmid (dPelican.attB.UAS_CYP4G16 and dPelican.attB.UAS_CYP4G17) contained also a mini-*white* marker for *Drosophila*. These plasmids were sequence verified using primers pPel_uas F/pPel_sv40 R (Table S1) and used to inject preblastoderm embryos of the *D. melanogaster* strain *y[1] M{vas-int.Dm}ZH-2A w[*]; PBac{y[+]-attP-9A}VK00013* (referred hereafter as VK13 strain, #24864 in Bloomington Drosophila Stock Center, kindly provided by M. Monastirioti and C. Delidakis, IMBB) which enables φC31 integrase expression under *vasa* promoter in chromosome X and bears an attP landing site in the 3rd chromosome. G_0 injected VK13 flies were crossed with *yw* flies and G_1 progeny was screened for w^+ phenotypes (red eyes) indicating integration of the recombinant plasmid. Independent transformed lines were crossed with a balancer strain for the 3rd chromosome (*yw*; TM3 *Sb*/TM6B *Tb Hu*) and G_2 flies with red eyes and relevant marker phenotype were selected and crossed among themselves to generate the homozygous flies used to establish the transgenic responder lines (Fig. S1).

2.7. Generation of flies used for rescue experiment

In order to generate flies where both oenocyte-specific *Drosophila* Cyp4g1 RNAi knock-down and *Anopheles CYP4G16* and/or *CYP4G17* expression by one or two transgene copies would take place, a series of standard genetic crosses (see Fig. S1 for detailed strategy) was performed in order to generate homozygous lines bearing either both RE-Gal4 (2nd chromosome) and UAS-*CYP4G16* or UAS-*CYP4G17* (3rd chromosome), or both UAS-*Cyp4g1*-KD (2nd chromosome) and UAS-*CYP4G16* or UAS-*CYP4G17* (3rd chromosome). Then, several different combinations of crosses provided all the genotypes used for rescue experiments as shown in Table S2.

2.8. Quantification of eclosion (adult survival and adult mortality)

For quantification experiments appropriate fly crosses were set up by crossing 5 virgin females with 5 males of the appropriate genotypes as shown in Table S2. 2nd instar larvae were collected and transferred into fly food in batches of 20 (approximately 130 larvae per biological replicate were transferred). Pupae were then counted to determine pupation efficiency and successfully eclosed adults were measured. To address eclosion we measured the alive adults (males and females), while newly emerged adults that died immediately after eclosion were counted separately in order to address the adult mortality, in three biological replicates.

2.9. Extraction of cuticular lipids, cuticular hydrocarbons (CHCs) fractionation, identification and quantitation

Crosses B x 2, B x 3, C x 3 and G x 1 (Table S2) were set up and the progeny (B2, B3, C3 and G1, Table S2) was separated by sex at emergence. One-day old male flies from each condition were dried at Room Temperature for at least 48 h. Approximately 150 flies of each condition were separated in 3 replicates, the dry weight of each replicate was measured and they were send for CHC analysis in VITAS-Analytical Services (Oslo, Norway). Briefly, cuticular lipids from all samples were extracted by 1-min immersion in hexane (x3) with gentle agitation; extracts were pooled and evaporated under a N_2 stream. CHCs were separated from other components and finally concentrated prior to chromatography by Solid Phase Extraction (SPE). CHC identification by gas chromatography-mass spectrometry (GC-MS) and CHC quantitation by GC-flame ionization detector (FID) were performed as described previously (Balabanidou et al., 2016; Girotti et al., 2012). Quantitative amounts were estimated by co-injection of nC24 as an internal standard (2890 ng/ml in hexane). CHC quantification was calculated as the sum of area of 32 peaks in total (peaks 3 and 4 were excluded due to background noise) and the relative amount (mean value ± SD) of each component was calculated by dividing the corresponding peak area by the total CHC peak area, using the internal standard. Shorthand nomenclature of CHCs used in the text and tables is as follows: CXX indicates the total number of carbons in the straight chain; linear alkanes are denoted as n-CXX; the location of methyl branches is described as x-Me for monomethyl-alkanes and as x,x-DiMe for dimethyl-alkanes. Alkenes are shown as x-CXX:1. Statistics were analyzed using GraphPad Prism software, version 6.01. Differences in the total CHC values were analyzed with Student's *t*-test.

2.10. Western blots

Abdominal walls from 4th instar larvae, 1–5 h old pupae, 20–24 h old pupae and 1-12 h-old adults were homogenized into a Homogenization Buffer, containing 8 M Urea, 50 mM Tris-HCl, pH 8.0 and 0.5% SDS. Polypeptides resolved by SDS-PAGE (10% acrylamide) were electro-transferred on nitrocellulose membrane (GE Healthcare, Whatman) and probed with anti-CYP4G16, anti-CYP4G17 at a dilution of 1:250 in TBS-Tween. Antibody binding was detected using goat anti-rabbit IgG coupled to horseradish peroxidase (Cell Signaling) (diluted 1:10,000 in 1% skimmed milk in TBS-Tween buffer), visualized using a horseradish peroxidase sensitive ECL Western blotting detection kit (GE Healthcare, Little Chalfont, Buckinghamshire, UK) and the result was

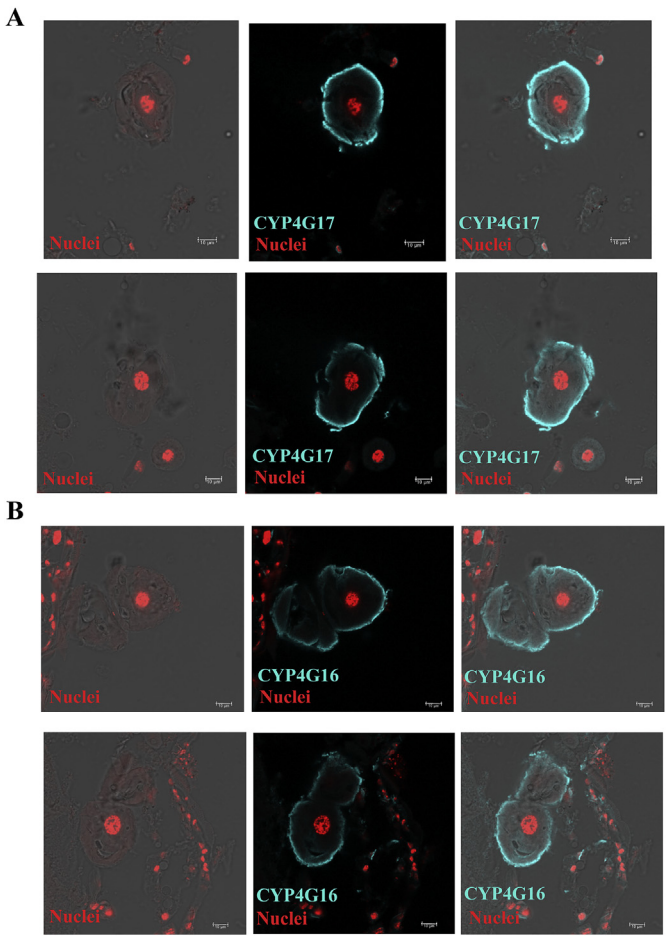

Fig. 1. Immunohistochemical localization of CYP4Gs in larvae. Merged immunohistochemical images from longitudinal sections of 4th instar mosquito larvae focusing on oenocytes. A) CYP4G17 peripheral localization in *An. gambiae* larval oneocytes, B) CYP4G16 peripheral localization in *An. gambiae* larval oenocytes. Cell nuclei are stained red with TOPRO; scale bars = 10 μm. *Left*: bright-field with stained nuclei, *middle*: antibody and nuclei staining, *right*: merge of bright-field, antibody and nuclei staining. (For interpretation of the references to color in this figure legend, the reader is referred to the Web version of this article.)

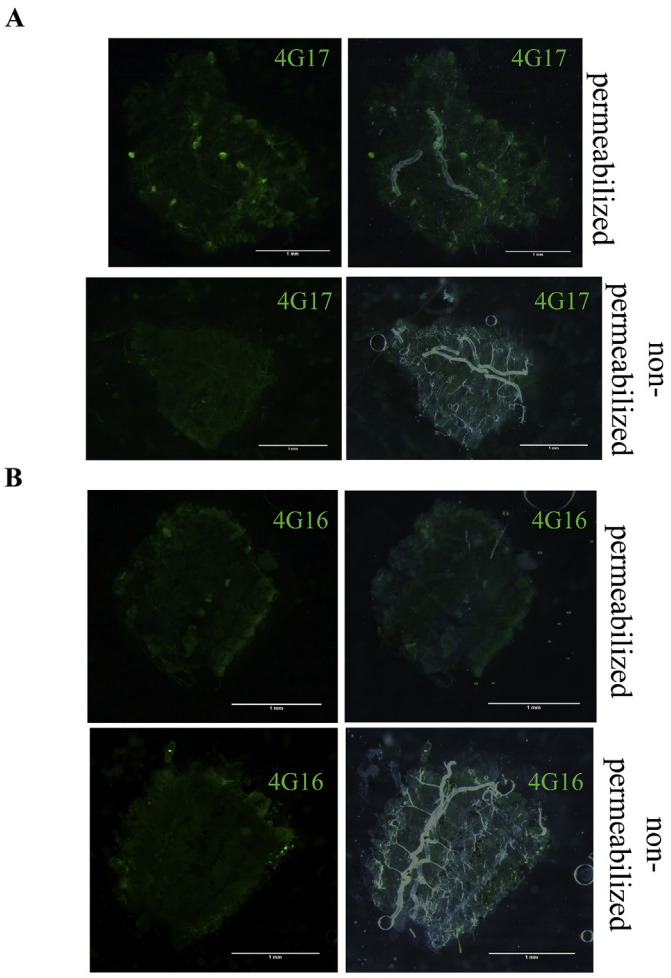

Fig. 2. Membrane topology of CYP4Gs. Immunohistochemical images from abdnominal walls (whole mounts) of 4thinstar mosquito larvae focusing on oenocytes. A) CYP4G17 and B) CYP4G16 in permeabilized and non-permeabilized conditions; scale bars = 1 mm.

recorded using Fujifilm LAS3000 CCD camera imaging station.

3. Results

3.1. Both CYP4G17 and CYP4G16 are anchored on the plasma membrane of 4th instar larval oenocytes with the globular part facing cytoplasmically

To determine the specific localization of CYP4G16 and CYP4G17 in 4th instar larvae, an immunohistochemistry approach was employed. Longitudinal sections from frozen pre-fixed mosquito specimens were immune-stained with anti-CYP4G17 and anti-CYP4G16 specific antibodies, respectively. CYP4G16 and CYP4G17 antibodies gave intense signals localizing in oenocytes. We were unable to detect specific signals in other tissues by immune-staining. Surprisingly, higher magnification confocal microscopy focusing on oenocytes revealed that both CYP4G17 and CYP4G16 are found at the periphery of the larval oenocytes, presumably associated with the plasma membrane (PM) (Fig. 1). According to topology prediction tools both proteins were predicted to have one transmembrane domain each. CYP4G16 and CYP4G17 transmembrane domains are predicted to span the residues seventeen to thirty nine and twenty to forty one respectively. Hence, in order to investigate the hypothesis that they span the membrane with one helix with the N-terminus located in the extracellular space of oenocyte cells, separated from the remainder globular part of the protein that is located intracellularly we performed immunohistochemical experiments in abdominal larval walls in permeabilized and non-permeabilized conditions (Fig. 2). The fact that specific antibodies used recognize epitopes closer to the C-termini of the proteins together with the absence of oenocyte-specific staining in non-permeabilized conditions for both CYP4G16 and CYP4G17 as well as *in silico* prediction strongly indicate that both are anchored on the plasma membrane, facing the cytoplasm, with their N-termini residing outside of the cell.

3.2. Two differentially localized CYP4G17 forms in pupal oenocytes, of larval and adult origin

To immunolocalize CYP4G17 and CYP4G16 in pupae, the same immunohistochemical approach in longitudinal cryosections in pupal abdominal walls was performed as above. In pupae, both CYP4G16 and CYP4G17 antibodies gave intense signals in two cell types. We detected both close to the lateral pupal cuticular walls. The larger cells, full of round-shaped vesicular structures and lipid droplets are the remaining larval oenocytes, while the smaller in size rounded-shaped cells that are also found singly and in clusters are the newly-developing adult oenocytes (Fig. 3). CYP4G16 maintained a peripheral localization in both oenocyte types (Fig. 3A and B), whereas CYP4G17 antibody gave localized signals of two distinct patterns. Peripheral staining (Fig. 3C) was

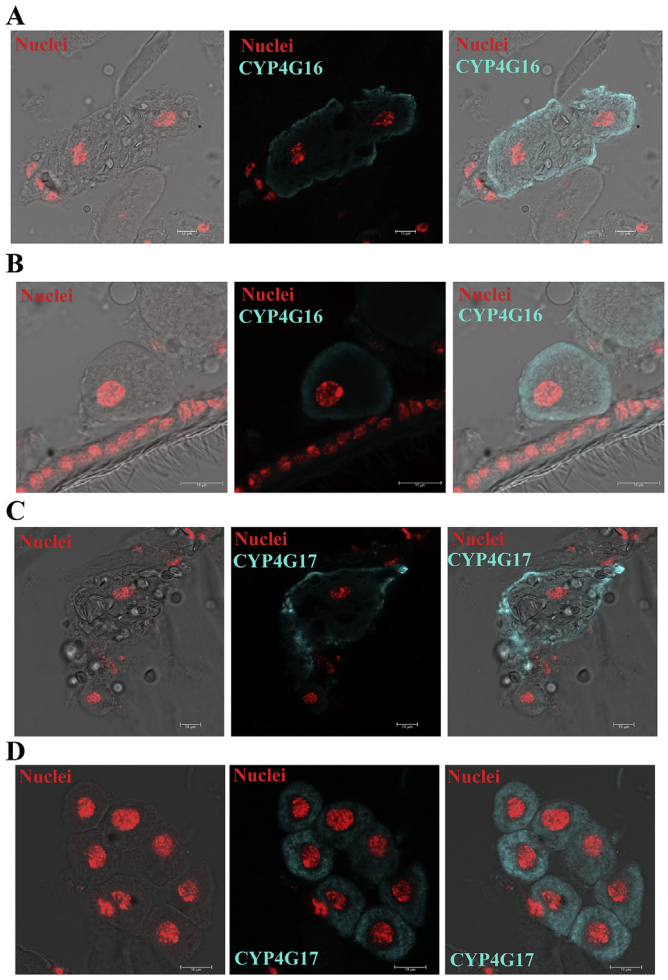

Fig. 3. Immunohistochemical localization of CYP4Gs in pupae. Merged immunohistochemical images from longitudinal sections of pupal abdominal walls. A) CYP4G16 localization in larval-origin pupal oenocytes mainly on the periphery of oenocytes, B) CYP4G16 localization in adult-origin pupal oenocytes mainly on the periphery, C) CYP4G17 localization in larval-origin pupal oenocytes mainly on the periphery of oenocytes, D) CYP4G17 localization in adult-origin, newly-developed oenocytes of pupae, forming a cluster, showing the protein dispersed throughout the cytoplasm. Cell nuclei are stained red with TOPRO; scale bars = 10 µm. *Left*: bright-field with stained nuclei, *middle*: antibody and nuclei staining, *right*: merge of bright-field, antibody and nuclei staining. (For interpretation of the references to color in this figure legend, the reader is referred to the Web version of this article.)

maintained in cells of larval origin, while the developing adult cells were stained with anti-CYP4G17 throughout their cytoplasm (Fig. 3D).

To further examine the different sub-cellular localization observed in the two types of oenocytes found in pupae, we performed Western blot analysis with anti-CYP4G17 using abdominal walls of 4th instar larvae, newly-formed pupae (1-5 h-old), pupae prior to emergence (20-24 h-old) and newly emerged adults (1-12 h-old). Interestingly, we observed two bands in different molecular sizes in all developmental stages with a difference in the intensity in each condition tested (Fig. 4). The lower band has a molecular mass of around 65 kDa, which is close to the estimated molecular mass of the protein (64 kDa), whereas the upper band migrates approximately at 70 kDa.

3.3. Oenocyte-specific expression of CYP4G16 and CYP4G17 in CYP4G1 knock-down Drosophila can restore viability

Using a series of genetic manipulations we were able to induce the expression of either or both mosquito CYP4Gs while simultaneously

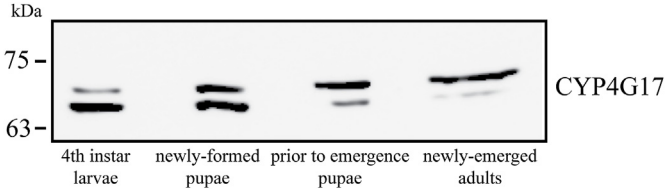

Fig. 4. Expression pattern of CYP4G17 among different *An. gambiae* developmental stages. Whole protein extracts from dissected abdominal walls of 4th instar larvae (lane 1), newly-formed pupae (lane 2), pupae prior to emergence (lane 3) and newly emerged adults (lane 4), were analyzed by Western blot using anti-CYP4G17.

silencing the endogenous *Cyp4g1* gene specifically in oenocytes (Fig. S1 and Table S2). Phenotypic analysis showed that all *Cyp4g1*-KD flies die at emergence, not being able to eclose from the pupal case. However, viability was almost completely restored in the presence of two copies of *CYP4G16* (with respective elevated transcripts 1.95 ± 0.4 - fold, $n = 3$, $p < 0.01$, compared to the single copy transgene flies) and of *CYP4G16* in combination with *CYP4G17* (Fig. S2). Quantitative analysis of all the different CYP4G conditions tested revealed that CYP4G16 and CYP4G17 exhibit differential ability to rescue the lethal phenotype in an oenocyte-specific *Cyp4g1* knock-down genetic background (Fig. 5). As shown in Figs. 5 86% of the larvae expressing *CYP4G16* in two copies successfully emerged into adults, while *CYP4G17* in two copies is able to rescue approximately 33% of the flies, revealing its ability to partially complement *Cyp4g1* silencing. This demonstrates that CYP4G17 is also a functional oxidative decarbonylase. The ability of each transgene to rescue the lethal phenotype is dose-dependent since *CYP4G16* in one copy only partially restores viability (15% survivors), while overexpression of one copy of *CYP4G17* seems to generate flies arrested during eclosion. However, the combination of *CYP4G16* and

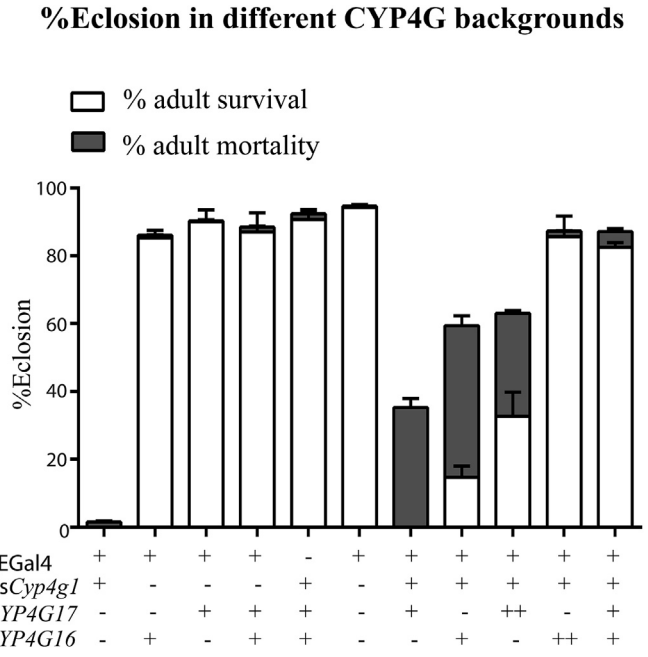

Fig. 5. Percent eclosion of *D. melanogaster* flies in different CYP4G backgrounds. Quantification of adult flies that successfully eclosed corresponding to a known number of pupae. White bars represent successfully eclosed adults that survived (%), while flies that died as newly-emerged adults lying on the food were calculated to address mortality post successful eclosion (%) and are depicted with grey bars. Different CYP4G backgrounds are described at the bottom of the graph with "+" representing the presence and "–" the absence of a P450 gene (*Cyp4g1*, *CYP4G17*, *and CYP4G16*) or the oenocyte-specific GAL4 driver (REGal4). Mean of 3 biological experiments +SEM.

CYP4G17 gives a high percentage of survivors (83%), similar to a double dose of *CYP4G16*. Interestingly, in cases of partial rescue (1x *CYP4G16* or 2x *CYP4G17*), as well as in the case of 1x *CYP4G17*, where no long time survivors are observed, a remarkable number of newly-emerged adults, mostly females, survive the eclosion burden but die almost immediately and are found lying dead on the food. This is in contrast to *Cyp4g1*-KD flies where only dead adults unable to fully exit the puparium were observed (Fig. 5 and S2). Moreover, in partially rescued CYP4G backgrounds (1x *CYP4G16* and 2x *CYP4G17*) the vast majority of successfully eclosed survivors (almost 80%) are males.

3.4. Three very long-chain dimethyl-branched CHCs are present in CYP4G16, CYP4G17 and CYP4G16/CYP4G17 flies, but not 'wild-type' CYP4G1 flies

After extraction of cuticular lipids and quantification, different total hydrocarbon amounts were identified per mg of dry weight in each condition tested (Fig. S3), with the control flies (no knock-down of *Cyp4g1*) having the highest total CHC content and the flies bearing the *CYP4G17* transgene in the absence of *Cyp4g1* the lowest (p-value < 0.001). CYP4G16/CYP4G17 and CYP4G16/CYP4G16 appeared to have approximately the same total CHC amount (non-significant difference) (Fig. S3). Moreover, 18 CHC compounds were identified in the control flies (no mosquito transgene) and 21 CHC compounds (18 similar and 3 extra) in the *D. melanogaster* flies expressing mosquito transgenes. Interestingly, the three extra CHCs present in all *Drosophila* strains expressing mosquito CYP4Gs but not in the control (CYP4G1) flies, corresponded to the three longer CHCs (dimethyl-C45, dimethyl-C46 and dimethyl-C47) identified (Fig. 6) often found in *Anopheles*. Additionally, the relative abundance of each CHC identified was calculated in % area and it was shown that CYP4G17 and CYP4G16/CYP4G17 produce significantly more of these three very-long chain dimethyl-branched compounds (Fig. 6) than CYP4G16. Other statistically significant differences indicate that C31 is more enriched in the presence of CYP4G17 rather than CYP4G16 (p-value < 0.001) and that C25 (p-value < 0.0001), C27 (p-value < 0.0001), methyl-C29 (p-value < 0.0001) and C31:1 (p-value < 0.001) are more abundant in CYP4G16 mosquitoes.

4. Discussion

The CYP4G are highly conserved P450 enzymes in insects and the discovery that they serve as oxidative decarbonylases in the last step of hydrocarbon biosynthesis (Qiu et al., 2012) was the first explanation provided for this high degree of conservation. However, much remains to be learned about these enzymes. In *Drosophila*, CYP4G1 is a major protein of oenocytes, whereas its paralog CYP4G15 is found in the brain (Maibeche-Coisne et al., 2000) where its function is unknown. In the major malaria vector *Anopheles gambiae* the situation is different, because both the CYP4G1 and CYP4G15 paralogues, named CYP4G17 and CYP4G16, are highly expressed in oenocytes (Balabanidou et al., 2016). This study further showed that while a CPR-CYP4G16 fusion was able to catalyze the oxidative decarbonylation of a C18 aldehyde, this activity was not detectable for CYP4G17 (Balabanidou et al., 2016). The two enzymes also differed in their subcellular localization in adult *An. gambiae* oenocytes (Balabanidou et al., 2016). The results presented here address both differences between CYP4G16 and CYP4G17.

In contrast to what is expected for microsomal P450s, CYP4G16 was previously shown to be present on the internal side of the PM in adult oenocytes (Balabanidou et al., 2016) and here we show that it has the same subcellular localization and topology in oenocytes from an earlier developmental stage and origin (Figs. 1B, 3A and 3B). In larval oenocytes, CYP4G17 also appears anchored to the PM (Figs. 1A and 3C). The N-terminus of each protein is predicted to be facing extracellularly with a transmembrane helix connecting to the catalytic part of the enzyme, shown to be on the cytoplasmic side (Fig. 2). In pupae, CYP4G17 is found to be dispersed throughout the cytoplasm in developing adult-type oenocytes (Fig. 3D) as we have observed previously in fully developed adults (Balabanidou et al., 2016). This difference in CYP4G17 localization is also accompanied by a difference in molecular weight, as indicated by Western blot analysis of different developmental stages (Fig. 4). One plausible scenario is that the two bands identified in Fig. 4 represent developmentally specific isoforms; under this scenario adult CYP4G17 (*ad*CYP4G17) may be modified by a yet unidentified pre- or post-translational mechanism, sufficient for the protein to be rendered to the ER as a typical ER-resident P450, while larval CYP4G17

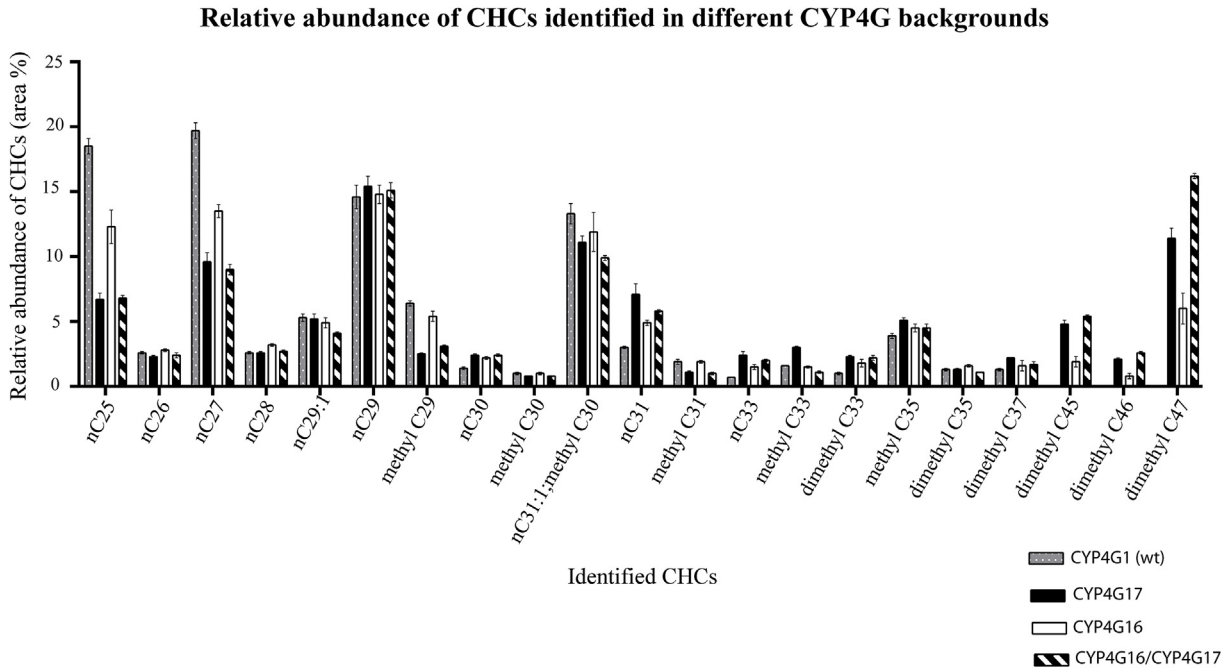

Fig. 6. Relative abundance of Cuticular Hydrocarbons (CHCs) identified in different CYP4G backgrounds. Relative CHCs abundances in % area are depicted for each one of the 21 out of 32 CHCs identified in total. Differentially colored bars correspond to the different CYP4G background present in each *Drosophila* strain analyzed (grey: G x 1, black: C x 3, white: B x 2 and black/white: B x 3 fly crosses as described in Table S2). Mean of 3 biological experiments ± SEM.

(*lar*CYP4G17) escapes the ER-rendering mechanism and is transported to the PM. Genomic sequence and transcript analysis does not indicate obvious alternative splicing, so we favor a post-translational modification that may be confirmed by proteomic analysis in future work. Under this hypothesis *lar* or *ad*CYP4G17 may also be functionally distinct. It is tempting to suggest that PM localization would favor export of CHC from the cell and transfer to lipophorin. However nothing is known yet of the physiology of intracellular CHC transport, and the localization of the upstream enzymes in oenocytes, desaturases and elongases, has been predicted but not verified.

The hypothesis of two different CYP4G17 isoforms is in line with the observation that the two different types of oenocytes co-exist in the mosquito pupa. It is known that in *D. melanogaster*, larval and adult generations of oenocytes are morphologically distinct ectodermal derivatives with separate developmental origins (Makki et al., 2014). In *An. gambiae* two distinct types of oenocytes have previously been found in larvae and adults stained for cytochrome P450 reductase (Lycett et al., 2006). Oenocyte functions seem to be closely related with molting, as a new generation of such cells is developed at each molt in some holometabolous species and the size and number of these cells can vary dramatically during *Drosophil*a larval development (Makki et al., 2014). Under our immunostaining approach in pupal abdomens, CYP4G17 and CYP4G16 oenocyte-specific intense staining revealed the morphological difference of oenocytes forms at this stage. Two distinct cell types that had similar morphologies to those described previously in larvae (Lycett et al., 2006) and adults (Balabanidou et al., 2016; Lycett et al., 2006) were found in pupae probably owing to the existence of two different origins of oenocytes in the pupal developmental stage. Big cells in size, carrying numerous bundles of lipid droplets are considered to be oenocytes of larval origin persisting in the pupal stage as they are very similar to those obtained in larvae longitudinal sections (Fig. 3A and C). Apart from these intense specific staining was obtained in smaller in size cells also found in clusters that are considered to be newly-developing oenocytes of adult-specificity (Fig. 3B and D).

Our previous biochemical analysis could not detect decarbonylase activity of CYP4G17 on short chain aldehydes, and so we have examined the comparative functions of the CYP4Gs by a genetic, *in vivo* approach. In this study, we performed the conditional expression of *An. gambiae* CYP4Gs in oenocytes of *Cyp4g1* knock-down *D. melanogaster* flies, in order to investigate if this expression could rescue the knock-down phenotype. Our results revealed that two copies of *CY4G16* or a *CYP4G16/CYP4G17* combination can almost completely restore the viability of *Cyp4g1*-KD flies, while one copy of *CYP4G16* and two copies of *CYP4G17* only lead to a partial rescue, indicating that both mosquito CYP4Gs can functionally substitute the fly decarbonylase, albeit to a different extent. Interestingly 1x *CYP4G17* showed almost zero levels of adult survival although a remarkable number of dead, early-emerged adults were found lying on the food in contrast to control *Cyp4g1*-KD flies (Fig. 5 and S2), which could not fully exit the puparium, implying that even the slight expression of *CYP4G17* (one allele present) results in better eclosion ability.

The results show that gene copy number (i.e. dose) affects survival ability. This is consistent with the very high expression level of native oenocyte CYP4Gs (Balabanidou et al., 2016; Chung et al., 2009), the sluggish enzyme activity observed *in vitro* until now (Balabanidou et al., 2016; Calla et al., 2018; Qiu et al., 2012) and the potentially lower level of activation provided by the RE driver. Interestingly, in cases of partial rescue (2x *CYP4G17* and 1x *CYP4G16*), males preferentially survive. Several studies on *Drosophila* species from temperate and tropical regions have shown a higher desiccation resistance of females than males (Parkash and Ranga, 2013). Perhaps, if females require more CHC for desiccation resistance, a deficit is more difficult to compensate. Alternatively, this may be the result of subtle differences in expression levels or spatiotemporal profile of the RE-Gal4 driver (Bousquet et al., 2012) between males and females that may affect CYP4G1 knock-down efficiency or specificity.

Since both *Anopheles* CYP4Gs can function as decarbonylases, we investigated the cuticular hydrocarbon profile of 'rescued' flies where CYP4G1 native expression in oenocytes has been knocked down and functionally substituted with one or both of the mosquito genes. In *Drosophila* oenocytes, CYP4G1 is the only oxidative decarbonylase, so the blend of CHC produced reflects the catalytic activity of a single enzyme on a large number of substrates that differ in length, saturation, and methyl branching. Its substrate specificity must therefore be quite broad. In the rescued flies, the total amount of hydrocarbons produced was somewhat lower than wild type. However, the pattern of hydrocarbons produced in flies rescued with alternative *Anopheles* 4Gs was different, indicating that the CYP4G enzymes may have a different substrate specificity to each other, and to the CYP4G1. In particular, three extra CHCs (dimethyl alkanes of very high MW) were detected in all cases where mosquito CYP4Gs (but not *Drosophila* CYP4G1) were present. These higher MW compounds are typically found on the *An. gambiae* cuticle (Balabanidou et al., 2016). The substrates for CYP4G enzymes are produced by a complex pathway of enzymes (ACCase, elongases, desaturases, acyl-CoA reductases), encoded by a large number of genes (Wicker-Thomas et al., 2015). It is the flux through those enzymes that determines the substrate pool for the CYP4G enzymes. Transport in the hemolymph (on lipophorins) and then through the epidermis and differential loss from the epicuticle then determines the blend of CHC that is measured. It is intriguing how these processes contribute to the apparition of higher MW CHCs not detected in wild type *Drosophila*. Although speculative, we propose several non-exclusive factors to explain this novel observation. On one hand, it is entirely plausible that the dimethyl-C45, -46 and −47 substrates are produced and converted to CHC in wild type *Drosophila* oenocytes at a level below detection in our assay. Indeed the classical GC method detects high MW CHC poorly and other methods are needed (Cvacka et al., 2006). On the other hand, in transgenic flies these substrates may be more efficiently converted by CYP4G16 and especially CYP4G17 than by CYP4G1. By drawing on the pool of high MW substrates, CYP4G17 (and CYP4G16) would increase their synthesis by relieving product inhibition of the Elovl elongases. Thus, more high MW substrates would become available in the transgenic flies than in the wild type flies. Furthermore, greater retention of the high MW CHC has been noted before (Qiu et al., 2012) so that both biochemical processes may contribute to the presence of dimethyl-C45, -46 and −47 alkanes in transgenic flies and allow their detection by our classical method. Our study therefore suggests that it is not only the activities of upstream enzymes in oenocytes that determines the blend of insect CHC (Qiu et al., 2012), but that substrate specificity of the last enzymes, the CYP4Gs, also contributes to it. This conclusion reaffirms the need to delineate CYP4G specificity, especially in insects that express more than one CYP4G gene in oenocytes.

Furthermore, the differential subcellular localization of CYP4G17 during development and its apparent ability to act as a more efficient decarbonylase of very long-chain dimethyl-branched compounds in *Drosophila* reveal an intriguing functional diversification of the *An. gambiae* CYP4Gs. Further studies will be aimed to elucidate the molecular mechanisms of differential localization of CYP4G17 in larval and adult oenocytes, and to delineate precisely the substrate specificity of each CYP4G enzyme.

Acknowledgements

This research is co-financed by Greece and the European Union (European Social Fund- ESF) through the Operational Programme "Human Resources Development, Education and Lifelong Learning" in the context of the project "Strengthening Human Resources Research Potential via Doctorate Research" (MIS-5000432), implemented by the Greek State Scholarships Foundation (IKY) as a scholarship to MK. The post-doctoral research of VB was supported by a fellowship from IKY (Greek State Scholarships Foundation) funded by the action "Support of

Post-Doctoral Researchers" from the Operational Program "Development of Human Resources, Education and Life-Long Learning" with priority areas 6, 8, 9 and co-funded by the European Social Fund – ECB and Greek public funds (MIS: 5001552), as well as the European Union's Horizon (INFRAVEC) research and innovation programme under *grant agreement* No 731060 to JV. We wish to thank Prof. Christos Delidakis and Dr. Maria Monastirioti (IMBB/FORTH) for providing fly strains and for useful discussions, as well as Pawel Piwko for kindly providing us a plasmid vector backbone, Ioannis Livadaras for performing injections in *Drosophila* embryos and Amalia Anthousi for initially testing the RE-Gal4 driver strain.

Appendix A. Supplementary data

Supplementary data to this article can be found online at https://doi.org/10.1016/j.ibmb.2019.04.018.

References

Arcaz, A.C., Huestis, D.L., Dao, A., Yaro, A.S., Diallo, M., Andersen, J., Blomquist, G.J., Lehmann, T., 2016. Desiccation tolerance in Anopheles coluzzii: the effects of spiracle size and cuticular hydrocarbons. J. Exp. Biol. 219, 1675–1688.

Balabanidou, V., Grigoraki, L., Vontas, J., 2018. Insect cuticle: a critical determinant of insecticide resistance. Curr Opin Insect Sci 27, 68–74.

Balabanidou, V., Kampouraki, A., MacLean, M., Blomquist, G.J., Tittiger, C., Juarez, M.P., Mijailovsky, S.J., Chalepakis, G., Anthousi, A., Lynd, A., Antoine, S., Hemingway, J., Ranson, H., Lycett, G.J., Vontas, J., 2016. Cytochrome P450 associated with insecticide resistance catalyzes cuticular hydrocarbon production in Anopheles gambiae. Proc. Natl. Acad. Sci. U. S. A. 113, 9268–9273.

Barolo, S., Carver, L.A., Posakony, J.W., 2000. GFP and beta-galactosidase transformation vectors for promoter/enhancer analysis in Drosophila. Biotechniques 29.

Billeter, J.C., Atallah, J., Krupp, J.J., Millar, J.G., Levine, J.D., 2009. Specialized cells tag sexual and species identity in Drosophila melanogaster. Nature 461, 987–991.

Bousquet, F., Nojima, T., Houot, B., Chauvel, I., Chaudy, S., Dupas, S., Yamamoto, D., Ferveur, J.F., 2012. Expression of a desaturase gene, desat1, in neural and nonneural tissues separately affects perception and emission of sex pheromones in Drosophila. Proc. Natl. Acad. Sci. U. S. A. 109, 249–254.

Calla, B., MacLean, M., Liao, L.H., Dhanjal, I., Tittiger, C., Blomquist, G.J., Berenbaum, M.R., 2018. Functional characterization of CYP4G11-a highly conserved enzyme in the western honey bee Apis mellifera. Insect Mol. Biol. 27, 661–674.

Caputo, B., Dani, F.R., Horne, G.L., Petrarca, V., Turillazzi, S., Coluzzi, M., Priestman, A.A., della Torre, A., 2005. Identification and composition of cuticular hydrocarbons of the major Afrotropical malaria vector Anopheles gambiae s.s. (Diptera: Culicidae): analysis of sexual dimorphism and age-related changes. J. Mass Spectrom. 40, 1595–1604.

Chung, H., Carroll, S.B., 2015. Wax, sex and the origin of species: dual roles of insect cuticular hydrocarbons in adaptation and mating. Bioessays 37, 822–830.

Chung, H., Loehlin, D.W., Dufour, H.D., Vaccarro, K., Millar, J.G., Carroll, S.B., 2014. A single gene affects both ecological divergence and mate choice in Drosophila. Science 343, 1148–1151.

Chung, H., Sztal, T., Pasricha, S., Sridhar, M., Batterham, P., Daborn, P.J., 2009. Characterization of Drosophila melanogaster cytochrome P450 genes. Proc. Natl. Acad. Sci. U. S. A. 106, 5731–5736.

Cocchiararo-Bastias, L.M., Mijailovsky, S.J., Calderon-Fernandez, G.M., Figueiras, A.N., Juarez, M.P., 2011. Epicuticle lipids mediate mate recognition in Triatoma infestans. J. Chem. Ecol. 37, 246–252.

Cvacka, J., Jiros, P., Sobotnik, J., Hanus, R., Svatos, A., 2006. Analysis of insect cuticular hydrocarbons using matrix-assisted laser desorption/ionization mass spectrometry. J. Chem. Ecol. 32, 409–434.

Edi, C.V.A., Koudou, B.G., Jones, C.M., Weetman, D., Ranson, H., 2012. Multiple-insecticide resistance in Anopheles gambiae mosquitoes, southern cote d'Ivoire. Emerg. Infect. Dis. 18, 1508–1511.

Fan, Y., Zurek, L., Dykstra, M.J., Schal, C., 2003. Hydrocarbon synthesis by enzymatically dissociated oenocytes of the abdominal integument of the German Cockroach, Blattella germanica. Naturwissenschaften 90, 121–126.

Feyereisen, R., 2006. Evolution of insect P450. Biochem. Soc. Trans. 34, 1252–1255.

Gibbs, A.G., 2011. Thermodynamics of cuticular transpiration. J. Insect Physiol. 57, 1066–1069.

Girotti, J.R., Mijailovsky, S.J., Juarez, M.P., 2012. Epicuticular hydrocarbons of the sugarcane borer Diatraea saccharalis (Lepidoptera: crambidae). Physiol. Entomol. 37, 266–277.

Groth, A.C., Fish, M., Nusse, R., Calos, M.P., 2004. Construction of transgenic Drosophila by using the site-specific integrase from phage phiC31. Genetics 166, 1775–1782.

Gutierrez, E., Wiggins, D., Fielding, B., Gould, A.P., 2007. Specialized hepatocyte-like cells regulate Drosophila lipid metabolism. Nature 445, 275–280.

Howard, R.W., Blomquist, G.J., 2005. Ecological, behavioral, and biochemical aspects of insect hydrocarbons. Annu. Rev. Entomol. 50, 371–393.

Ingham, V.A., Jones, C.M., Pignatelli, P., Balabanidou, V., Vontas, J., Wagstaff, S.C., Moore, J.D., Ranson, H., 2014. Dissecting the organ specificity of insecticide resistance candidate genes in Anopheles gambiae: known and novel candidate genes. BMC Genomics 15, 1018.

Kall, L., Krogh, A., Sonnhammer, E.L., 2007. Advantages of combined transmembrane topology and signal peptide prediction–the Phobius web server. Nucleic Acids Res. 35, 5.

Lycett, G.J., McLaughlin, L.A., Ranson, H., Hemingway, J., Kafatos, F.C., Loukeris, T.G., Paine, M.J., 2006. Anopheles gambiae P450 reductase is highly expressed in oenocytes and in vivo knockdown increases permethrin susceptibility. Insect Mol. Biol. 15, 321–327.

MacLean, M., Nadeau, J., Gurnea, T., Tittiger, C., Blomquist, G.J., 2018. Mountain pine beetle (Dendroctonus ponderosae) CYP4Gs convert long and short chain alcohols and aldehydes to hydrocarbons. Insect Biochem. Mol. Biol. 102, 11–20.

Maibeche-Coisne, M., Monti-Dedieu, L., Aragon, S., Dauphin-Villemant, C., 2000. A new cytochrome P450 from Drosophila melanogaster, CYP4G15, expressed in the nervous system. Biochem. Biophys. Res. Commun. 273, 1132–1137.

Makki, R., Cinnamon, E., Gould, A.P., 2014. The development and functions of oenocytes. Annu. Rev. Entomol. 59, 405–425.

Parkash, R., Ranga, P., 2013. Sex-specific divergence for adaptations to dehydration stress in Drosophila kikkawai. J. Exp. Biol. 216, 3301–3313.

Parvy, J.P., Napal, L., Rubin, T., Poidevin, M., Perrin, L., Wicker-Thomas, C., Montagne, J., 2012. Drosophila melanogaster Acetyl-CoA-carboxylase sustains a fatty acid-dependent remote signal to waterproof the respiratory system. PLoS Genet. 8, 30.

Piwko, P., Vitsaki, I., Livadaras, I., Delidakis, C., 2019. The role of insulators in transgene transvection in Drosophila. Genetics 302165. https://doi.org/10.1534/genetics.119.302165 (in press).

Qiu, Y., Tittiger, C., Wicker-Thomas, C., Le Goff, G., Young, S., Wajnberg, E., Fricaux, T., Taquet, N., Blomquist, G.J., Feyereisen, R., 2012. An insect-specific P450 oxidative decarbonylase for cuticular hydrocarbon biosynthesis. Proc. Natl. Acad. Sci. U. S. A. 109, 14858–14863.

Tsakireli, D., Riga, M., Kounadi, S., Douris, V., Vontas, J., 2019. Functional characterization of CYP6A51, a cytochrome P450 associated with pyrethroid resistance in the Mediterranean fruit fly Ceratitis capitata. Pestic. Biochem. Physiol. https://doi.org/10.1016/j.pestbp.2019.03.022 (in press).

Wicker-Thomas, C., Garrido, D., Bontonou, G., Napal, L., Mazuras, N., Denis, B., Rubin, T., Parvy, J.P., Montagne, J., 2015. Flexible origin of hydrocarbon/pheromone precursors in Drosophila melanogaster. J. Lipid Res. 56, 2094–2101.

Wigglesworth, V.B., 1988. The source of lipids and polyphenols for the insect cuticle: the role of fat body, oenocytes and oenocytoids. Tissue Cell 20, 919–932.